

## **Travel path uncertainty : a case study combining stochastic and deterministic hydrodynamic models in the Rhône valley, Switzerland**

Francesco Kimmeier<sup>1</sup>, Mahmoud Bouzelboudjen<sup>1</sup>, Rachid Ababou<sup>2</sup>, Luis Ribeiro<sup>3</sup>

<sup>1</sup> CHYN - Centre d'Hydrogéologie, Université de Neuchâtel, Emile-Argand 11, 2007 Neuchâtel, Suisse

<sup>2</sup> IMFT - Institut de Mécanique des Fluides de Toulouse, Allée C. Soula, 31400 Toulouse, France

<sup>3</sup> CVRM-Instituto Superior Técnico, av. Rovisco Pais, 1049-001 Lisboa, Portugal

### **ABSTRACT**

In the framework of waste storage in geological formations at shallow or greater depths and accidental pollution, the numerical simulation of groundwater flow and contaminant transport represents an important instrument to predict and quantify the pollution as a function of time and space. The numerical simulation problem, and the required hydrogeologic data, are often approached in a deterministic fashion. However, deterministic models do not allow to evaluate the uncertainty of results. Furthermore, the hydrogeologic data and hydrodynamic properties required to implement the flow-transport model are generally very scant, so that an essential part of the simulation effort needs to be devoted to building the different spatially distributed data through spatial interpolation, extrapolation, smoothing, etc. In this paper, deterministic (classic finite element hydrodynamic model) and stochastic approaches (geostatistics: kriging and conditional simulations) are used for evaluating groundwater flow patterns and pollutant trajectories for a site-specific application (Rhône valley aquifer in Switzerland, area of 6.5 km<sup>2</sup>). The stochastic approach, based on kriging and multiple conditional simulations, leads to a quantification of uncertainty of flow-transport simulations, which are due to the underlying uncertainty of hydrogeologic properties and their spatial distribution. The available data used in this case study are : 55 transmissivity, 791 permeability and 145 hydraulic potential values. In spite of the relative wealth of available data, our study shows that the uncertainty of pollutant migration pathlines and travel distances is relatively important. The distance traveled by a pollutant particle during 30 months varies between 3150 m and 4800 m over five different but equally plausible scenarios (conditional simulations). The uncertainty is about 42% relative to the average travel distance, or 55% relative to the smallest travel distance mentioned above.

**Keywords :** Kriging, conditional simulation, travel path uncertainty, hydrodynamic modeling.

### **1. INTRODUCTION**

In the area of environmental and subsurface pollution, hydrogeologists and engineers are mainly concerned with the problem of predicting pollutant migration

and identifying pollution sources, which is an essential prerequisite for the development of efficient planning tools (scenarios) and remediation strategies (management). To address these challenges, scientists must first analyse all the available data in order to estimate, in particular, the hydrodynamic parameters of the geological formations which affect groundwater flow and migration of dissolved chemical species migration. However, these hydrogeologic parameters are extremely variable in space, and difficult to measure accurately at many points. For example, local values of hydraulic permeability in an aquifer are often not known or only very roughly (say within one order of magnitude). In general, therefore, a precise estimation of spatially distributed parameters like hydraulic permeability is indeed very difficult to obtain [Schafmeister and Peckdeger, 1992].

The spatially distributed estimation problem can be attacked by geostatistical methods [Cressie, 1993; Chilès & Delfiner, 1999] which are able to determine "the best" possible estimation considering the available information, and also, to estimate the confidence intervals associated with this estimation [Matheron 1970; Delhomme 1979; Chilès and Delfiner 1999]. In particular, geostatistical methods based on kriging and random field simulations [Chauvet 1992; Ababou & al. 1994] can be used to estimate the uncertainty of the parameters via root-means-square errors. Furthermore, they can be used to generate several equally plausible replicates of the parameters taking both their spatial distribution and their uncertainty into account. Consequently, these methods are very useful for developing optimal strategies for the management of water resources [Ribeiro and Muge, 1989], optimizing and reducing the cost of observation networks [Rouhani 1990; Kitanidis 1997; Jaquet & al., 2000], and designing the protection of groundwater catchments [Vassolo & al., 1998].

This paper illustrates this type of approach for a specific site located in the Rhône valley, Valais, Switzerland (Annex 1). The aquifers of the Rhône valley in Switzerland are of great economic importance. The groundwaters connected to the Rhône river can easily be reached and are therefore exploitable at modest costs. However, the situation of these aquifers located in narrow valleys with intense human activity (industries, agriculture, railways, roads and highways) makes them especially vulnerable in terms of water quality (industrial and/or agricultural pollution) as well as quantity (local or regional disorders).

## **2. MATERIALS AND METHODS**

Since 1995, the swiss canton of Valais has decided to compile datasets from a number of local studies (water supply, hydro-electricity, and geotechnical studies) into a regional, integrated hydrogeological framework. The management of contaminated sites in Switzerland – and in the canton of Valais in particular has now become a major concern in the area of water resource protection. Indeed, a new legislation (OEaux 1998) now requires the delineation of the zone of influence of all water catchments of public interest that are vulnerable to pollution.

Our study area is located in a 6.5 km<sup>2</sup> area of the Rhône valley, approximately 8 km long and 0.8 km wide, located near the town of Visp on the alluvial plain of the Rhône Valais (Fig. 1). The area is a very vulnerable zone due to the presence of the Lonza industry (a chemical fertilizer factory) situated near the town of Visp which includes in particular a chemical waste repository (Fig. 1). The groundwater flow in the aquifer is strongly conditioned by the surface flow in the river (Rhône) and in the canals (Brigerbadkanal and Grossgrundkanal). The valley deposits consist of

quaternary sediments of glacial (recessional and lateral moraine), lacustrine, and fluvial origins. Rhône valley gravel alluvium forms the main aquifer of the region. The distribution of the different lithological formations to model is shown in Fig. 1 in the right inset, representing the vertical cross-section AB along the valley. From the top to the bottom the different formations are : shallow silts with an average thickness of 10 m (absent in some places), an upper gravel unit with an average thickness of 16 m (10 to 19 m), middle silts, which are never more 20 m thick (and are absent in some places) and overlying a lower gravel formation (average thickness 20 m).

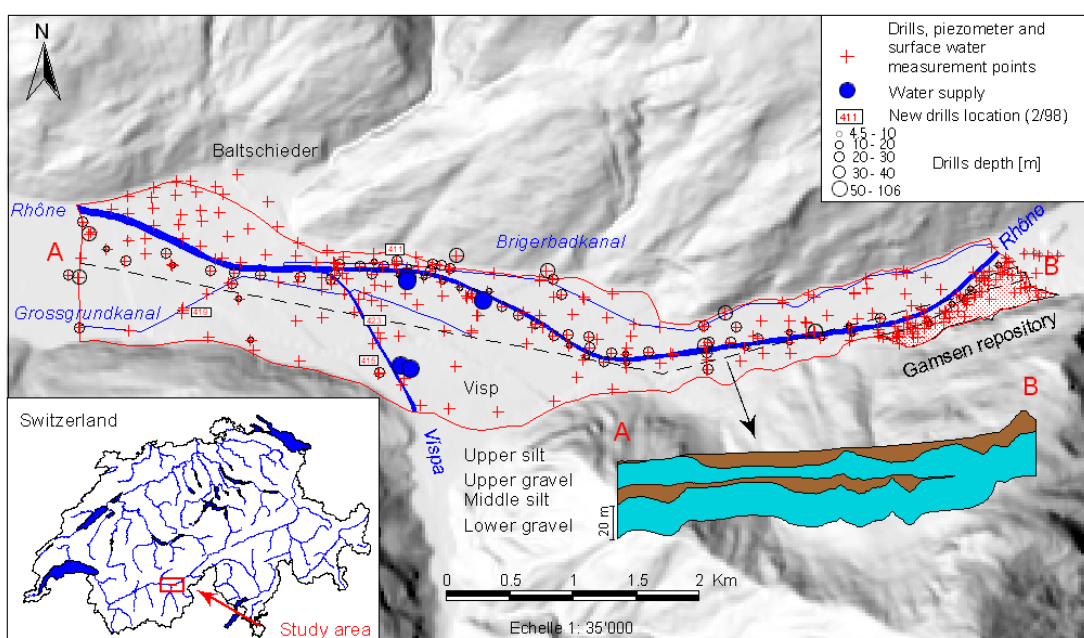


Figure 1 : Digital Elevation Model (DEM) of the Rhône valley between Gamsen and Baltschieder, Valais, Switzerland. The symbols show the positions of 144 drill points, 386 piezometers, and 23 surface water measurement points. The left inset shows the situation of the study area on a hydrographic map of Switzerland. The right inset displays the lithology of a vertical cross-section (AB) along the valley.

The dataset used in this study is relatively important in terms of number and quality of data. In particular it includes :

- 145 measurements of hydraulic potential  $H$  (m) in the upper partially confined aquifer, from 145 piezometers that are more or less evenly distributed in both the axial and transverse directions of the valley;
- 55 values of transmissivity  $T$  ( $\text{m}^2/\text{s}$ ) located mainly along the Rhône river; this implies that the spatial distribution of transmissivity is effectively known only along the 1-D axis of the valley (parallel to the river) and not across the valley. The preferential orientation is due to the fact that the drilling location were related to the proposed position of a highway parallel to the river.

In this work, a structural analysis (basic statistics and variography) of both hydrodynamic variables  $H$  and  $T$  discussed above was first conducted. Geostatistical techniques (kriging) were then applied to obtain an optimal estimation of aquifer properties, and stochastic conditional simulations were conducted to generate multiple replicates of aquifer properties, groundwater flow patterns, and pollutant migration pathlines. A "classical" deterministic model of groundwater flow (finite element method) was used to simulate groundwater flow for a given spatial distribution of

transmissivities. The combination of deterministic and stochastic hydrodynamic modeling allows a better characterisation of the spatial heterogeneity associated with the uncertainty of groundwater flow parameters given the available dataset.

It should be emphasized that the Rhône valley aquifers had only hitherto been studied, using deterministic models only. These models were used for assessing the future impact of the planned highway [Bouzelboudjen and Király, 1989], the impact of a potential pollution from the Gamsen repository depicted in Fig. 1 [Rossier, 1990], and the required correction of the Rhône riverbed [Kimmeier & al., 2000].

Fig. 1 shows the spatial database used within the framework of this study. The locations of the 144 boreholes, 386 piezometers and 23 surface water measurement points are presented. The boreholes are represented with symbols proportional to their depth. On the Fig. 2 and 5 we can see the 55 measurements of transmissivity and 145 of hydraulic potential.

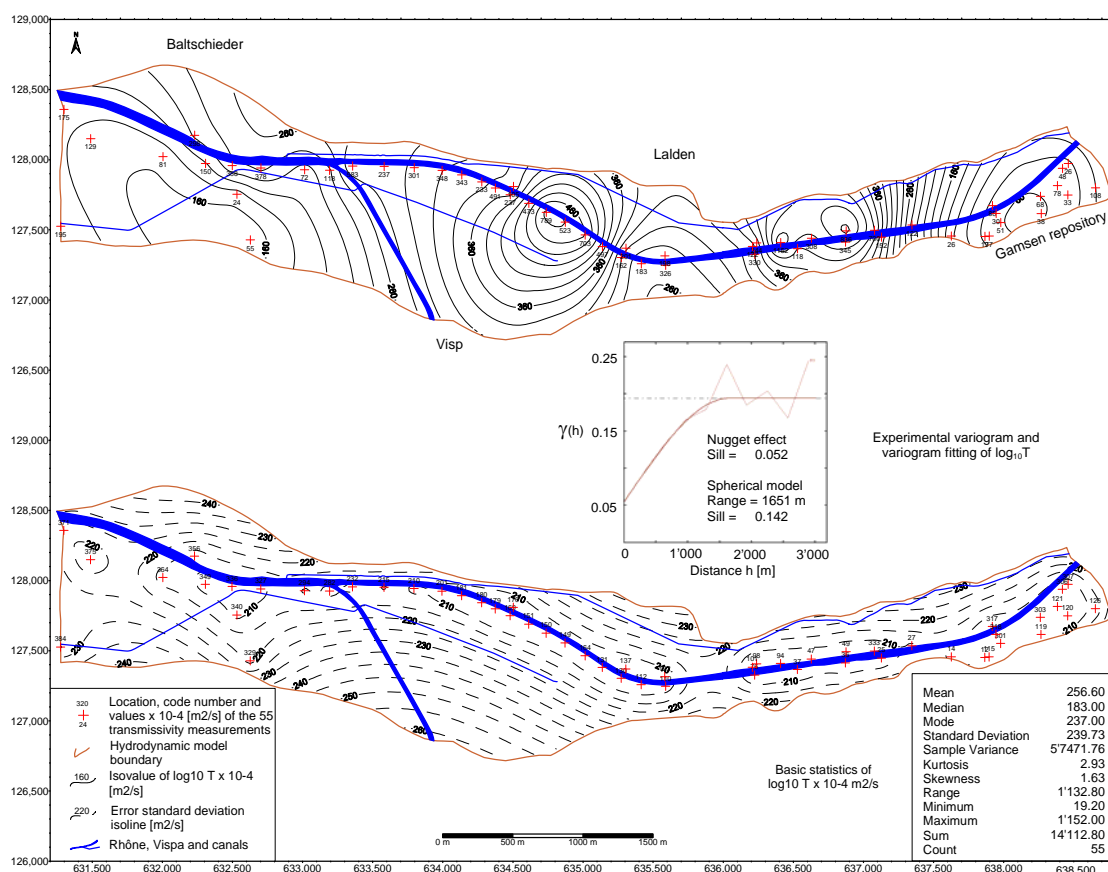


Figure 2 : Kriging maps of log-transmissivity field  $\log_{10}T$  in the Rhône valley study area. The contour map of estimated (kriged) log-transmissivity is displayed above, and the contour map of root-mean-square estimation error  $\epsilon_{\log T}$  is shown below. The numbers indicate isovalues of  $\log_{10}T$  (above) or  $\epsilon_{\log T}$  (below), with  $T$  given in  $10^{-4} \text{ m}^2/\text{s}$  units.

## 2.1 The geostatistical approach

To calculate the hydraulic potential ( $H$ ) fields and velocity fields by means of a hydrodynamic model, preliminary knowledge of the transmissivity ( $T$ ) field is necessary. The direct knowledge of this field can be only partial. To reconstruct the  $T$  and  $H$  fields we used a probabilistic approach developed by Matheron [1970] and applied to the water sciences by Delhomme [1979]. The term "regionalized" was

proposed by Matheron [1970] to qualify a phenomenon developing in the space (and/or in the time) and showing a certain structure. We treated regionalized variables by using the probabilistic theory of the random functions and interprets the regionalized variable as a "realization of the random function" [Delhomme, 1979]. The work of interrogation of the data, then the modelling of their structural properties, establishes under the name of variographic analysis the inescapable phase of any concrete geostatistical study [Chauvet, 1992].

In the probabilistic models, the simplest tool to measure a estimator quality is the variance. One makes the hypothesis that for a vector  $h$ , the increase  $Z(x + h) - Z(x)$  has an expected value and a variance independent at the point  $x$ , it is the intrinsic hypothesis :

$$E[Z(x + h) - Z(x)] = 0 \quad (1)$$

$$Var[Z(x + h) - Z(x)] = 2\gamma(h) \quad (2)$$

The function  $\gamma(h)$  is called semi-variogram. The semi-variogram is calculated by :

$$\gamma(h) = \frac{1}{2N(h)} \sum_{i=1}^{N(h)} [(z(x_i + h) - z(x_i))^2] \quad (3)$$

$z(x_i)$  are the data,  $x_i$  the points for which the data are available at the same moment in  $x_i$  and  $x_i + h$  and  $N(h)$  is the number of couples of points distant from  $h$ . In any geostatistical study the hypothesis of stationarity and ergodicity should be verified to allow correct estimations [Chauvet, 1992]. Having fitted a model to the experimental variogram , an estimation of our variable can be made at all points of a regular grid by the method of the standard kriging [Geostatistics, 1998].

There are other estimation methods taking into account the non-stationarity of the phenomenon (universal kriging, Intrinsic Random Function of order  $k$  : IRF- $k$ ), [Chauvet, 1992].

Simulations represent other methods of estimation which reconstruct the real variability of the variable and allow to calculate probability maps [Chilès and Delfiner, 1999]. If  $Z(x)$  is the studied regionalized variable, which we consider as a realization of a IRF- $k$ , and which is known only at  $n$  points  $x$ , one calls conditional simulation of  $Z(x)$  any realization  $T(x)$  of the same IRF- $k$  that passes by the data at points  $x$ . A conditional simulation is thus characterized by both following properties : it has the same generalized covariance as the phenomenon considered, and it passes through the experimental points.

Although the conditional simulations are not good estimators of the real field (the best estimator being the kriging) they are possible variants of the real field presenting the same degree of variability, respecting what one knows of the real field. They allow to surround the possible fluctuations in the phenomenon [Tompson and al., 1989] better than do the kriging (which smooths the reality) and the standard deviation of kriging (which does not give indication on the spatial structure of the error of estimation). They remain however connected to the kriging : if one builds a great number of conditional simulations, the average of their values at a point will restore the estimated value by kriging, and their variance of corresponding estimation.

## 2.2 The 2-D groundwater modeling approach

Finite element numerical models are particularly well suited to simulate groundwater flow in heterogeneous media. The 2-D saturated, constant density, steady state groundwater flow is represented by equation 4 :

$$\text{div}\left(-\overline{T} \cdot \vec{\text{grad}} h\right) + q = 0 \quad (4)$$

where  $\overline{T}$  is the hydraulic transmissivity tensor [ $\text{m}^2 \cdot \text{s}^{-1}$ ],  $h$  is the hydraulic head [m], and  $q$  represents the general source/sink term [ $\text{m}^3/\text{s} \cdot \text{m}^2$ ] (infiltration, well discharge, etc.).

For this study the finite-element simulation system Feflow [Diersch, 1999] was used to model groundwater flow and transport processes for the calculation of the 2-D flow system, velocity field, trajectories and travel distances in steady state flow.

The necessary data for the calculation are the geometry of elements, the transmissivity for every element and boundary conditions.

## 3. APPLICATION AND RESULTS

### 3.1 Transmissivity field reconstruction by kriging and conditional simulations

Both kriging and conditional simulations were used to study the influence of the spatial variability of transmissivity on the groundwater flow. Based on the 55 values of transmissivity of the upper gravels, the following statistics are obtained:  $25.7 \times 10^{-3} \text{ m}^2/\text{s}$  for the average,  $1.9 \times 10^{-3} \text{ m}^2/\text{s}$  for the minimum, and  $115.2 \times 10^{-3} \text{ m}^2/\text{s}$  for the maximum. The logarithm of the transmissivity was used to calculate the experimental omnidirectional variogram (no detectable anisotropy) presenting a nugget effect (sill = 0.05). A spherical model (range = 1651 m, sill = 0.14) was fitted on the experimental model (Fig. 2) at the maximal variance (0.19).

First, the 55 values of transmissivity were regionalized on a grid of 25 x 25 m by using the method of the standard kriging with Isatis software [Geostatistics, 1998] allowing the mapping of the estimated variable and the error of estimation.

Secondly, conditional simulations were realized, by the method of Turning bands (1000 bands) [Delhomme, 1979], to generate five likely fields of log-transmissivity  $\log_{10}T$  [ $10^{-4} \text{ m}^2/\text{s}$ ] on a grid of 25 x 25 m (Fig. 3). Comparison of the results of the conditional simulations reveals that the five histograms and experimental variograms are similar (Fig. 4). Moreover the average and the standard deviation of every simulation is comparable to the average and to the standard deviation of the 55 transmissivity values.

### 3.2 Hydraulic potential field reconstruction by kriging

In order to impose to the hydrodynamic finite element model the hydraulic potential at the boundaries (upstream, downstream, and hydrographic system in connection with the aquifer [Bouzelboudjen, Király, 1989], Fig. 1 and 6) the variable hydraulic potential was regionalized by kriging (Fig. 5). The basic statistics for the

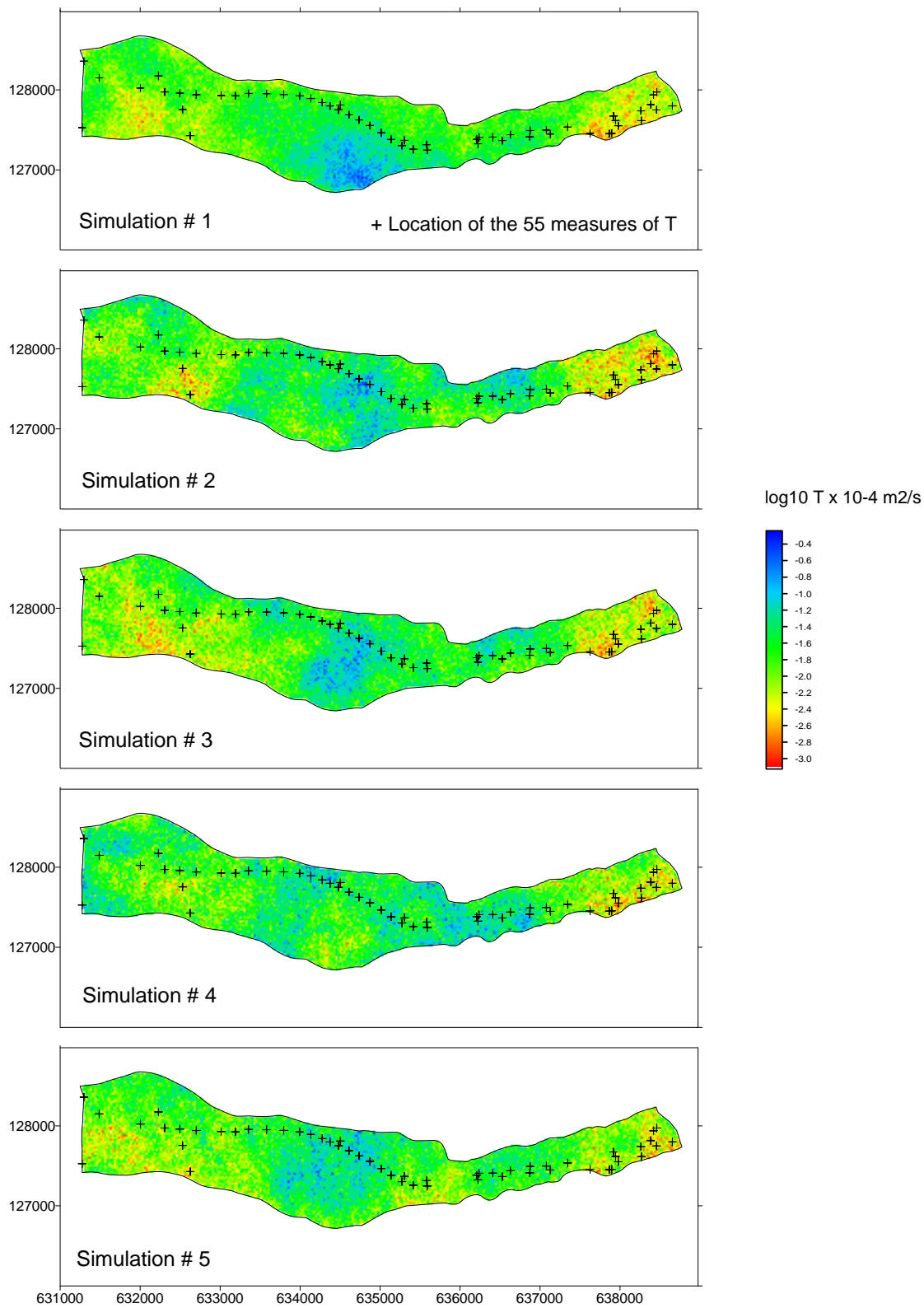


Figure 3 : Color maps of 5 replicates of the log-transmissivity field  $\log_{10} T [10^{-4} \text{ m}^2/\text{s}]$  in the upper gravel aquifer, obtained by conditional simulations with the Turning Bands method. The conditional simulation grid is 25 m x 25 m. The crosses indicate the location of the data.

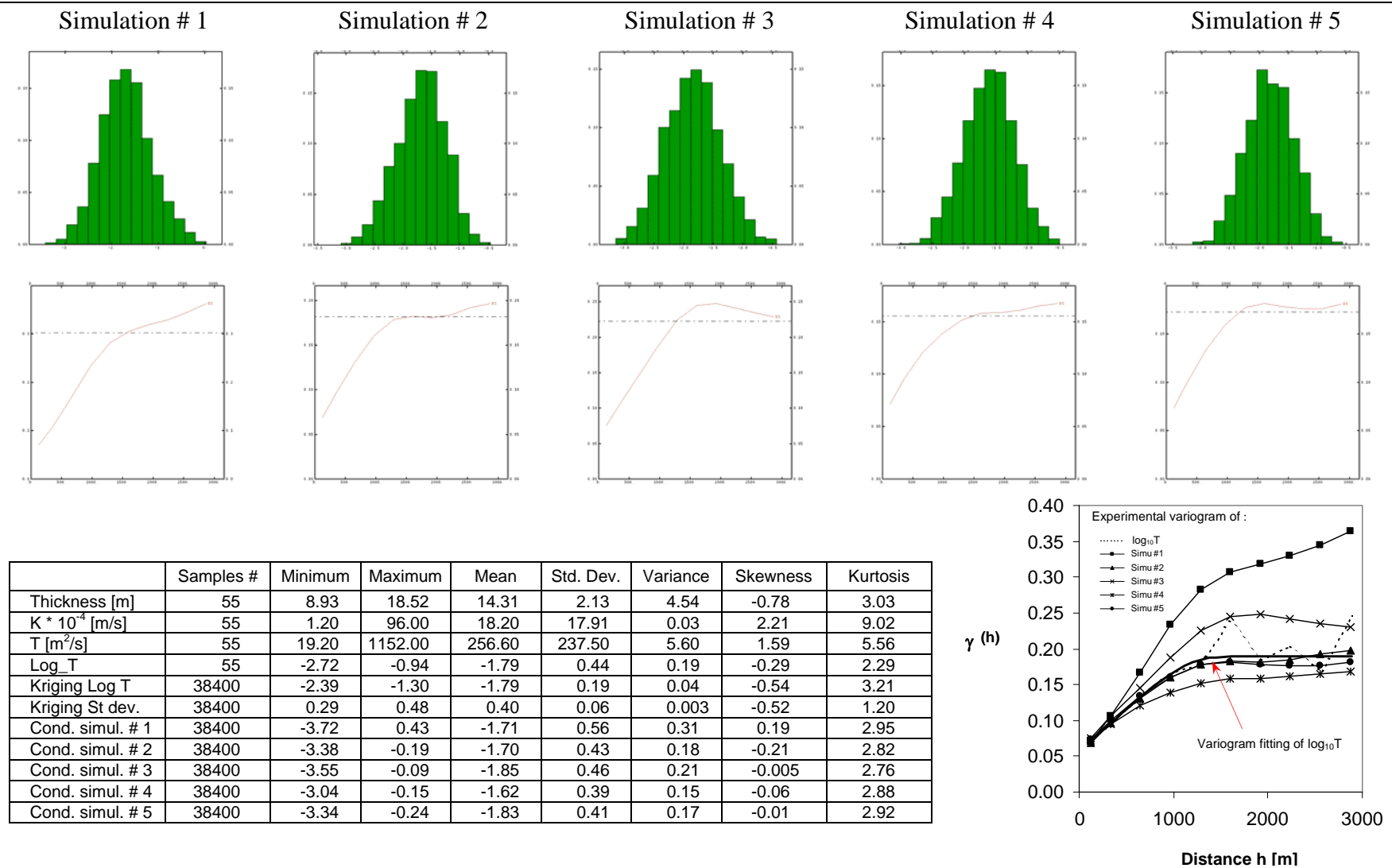


Figure 4 : Single-point and two-point statistics of the 5 simulated log-transmissivity field replicates :  $\log_{10}T$  histograms (top), experimental  $\log_{10}T$  variograms (middle), single-point moments of T and  $\log_{10}T$  (table at bottom left), and superimposed experimental variograms of the 5  $\log_{10}T$  replicates (bottom right). Variogram distances "h" are given in meters.

145 values of hydraulic potential are : 646.1 m for the average, 638.5 m for the minimum and 655.7 m for the maximum. The hydraulic potential variogram presents non-stationary spatial behavior characterized by a parabolic increase. It does not stabilise at great distance reflecting the presence of a drift (Fig. 5). The recognition of structures is indirect and is made automatically in two steps [Geovariances, 1998]. The first step consists in determining the degree of the drift by least-squares method. The second step consists in adjusting models of covariance generalized by iterative regression and selection of the optimal model. The hydraulic potentials were regionalized on a grid of 25 x 25 m using the method of the Isatis standard kriging. The moving neighborhood method of kriging allows an interpolation which takes into account the local variations of the hydraulic potential.

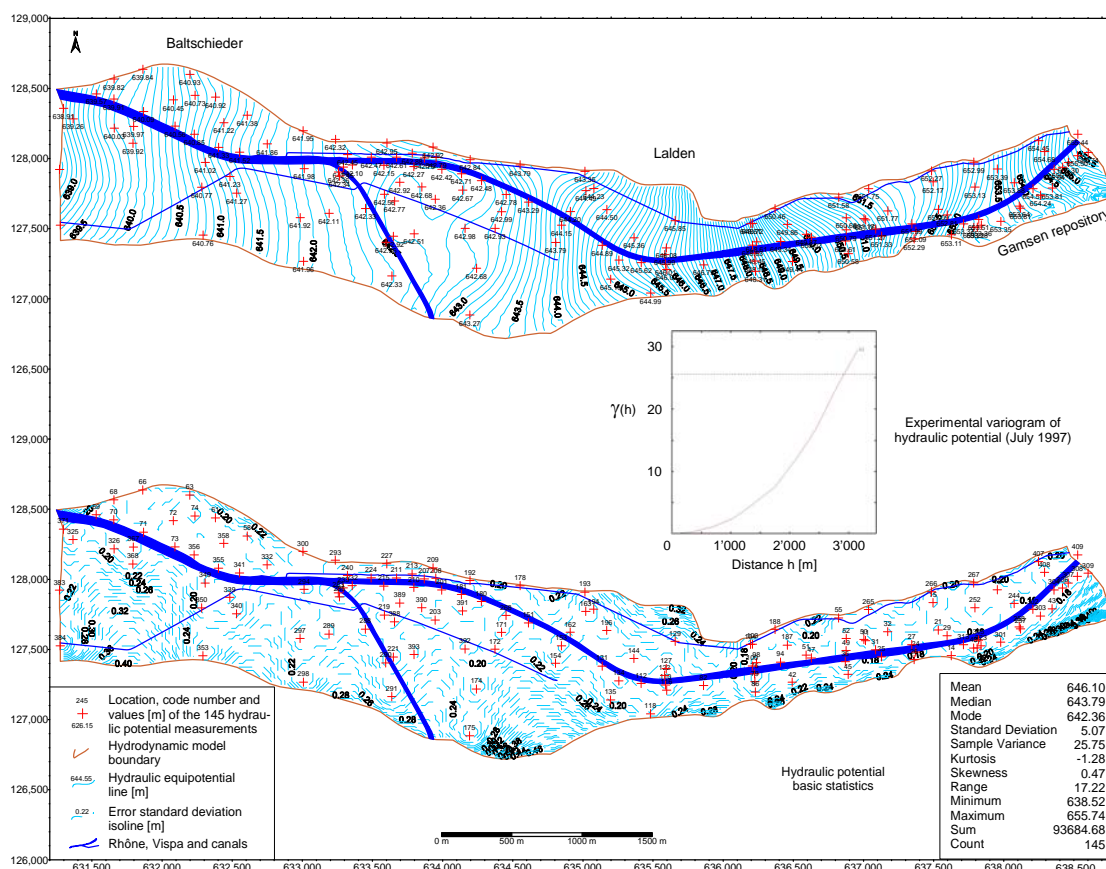


Figure 5 : Kriging contour maps of hydraulic potentials  $H$  (high water July 1997) in the upper gravel aquifer of the Rhône valley study area. The map of estimated (kriged) potential  $H$  is shown above, and the root-mean-square estimation error  $\varepsilon_H$  is shown below. The numbers indicate isovalues of estimated  $H$  (above) and of error  $\varepsilon_H$  (below) in meters. The histogram and variogram of hydraulic potentials are also depicted (insets).

### 3.3 Analyze of hydrodynamic model results

Fig. 6 shows the 2-D network of triangular finite elements for the mathematical hydrodynamic model as well as the nodes where the hydraulic potential were imposed along the Rhône river, along canals, and at the upstream and downstream boundaries (values issued of the map of estimated hydraulic potential by geostatistics, Fig. 5). The lateral boundaries are considered as no flow boundaries. After transformation of  $\log_{10}T$  to  $T$ , the various fields of transmissivity were assigned at the elements of the hydrodynamic model to obtain calculated hydraulic potential and velocity fields.

Fig. 6 also shows the results of one calculation of the distribution of calculated hydraulic potential by hydrodynamic model (simulation #1). It is interesting to compare the fields of hydraulic potential obtained by both methods (geostatistics and hydrodynamic models, Fig. 5 and 6). They show a similar distribution in their general presentation. The only problem not taken into account in the geostatistical simulations is the boundary conditions.

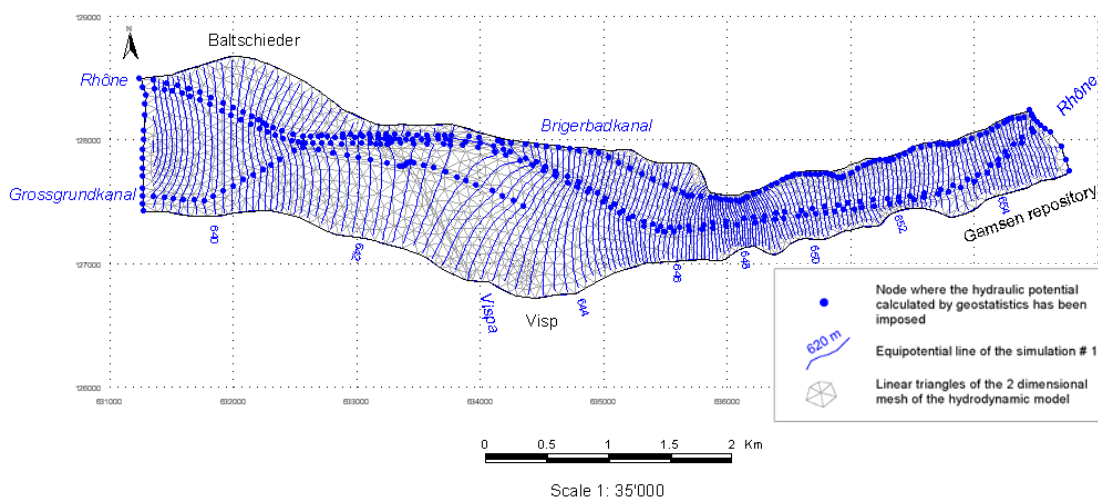


Figure 6 : Two-dimensional contour map of the calculated hydraulic potentials  $H$  obtained from groundwater flow simulation #1. The potential contours are superimposed on the 2D triangular mesh of the hydrodynamic model. The full circle symbols indicate upstream-downstream boundary conditions and "internal" river conditions (imposed hydraulic potentials).

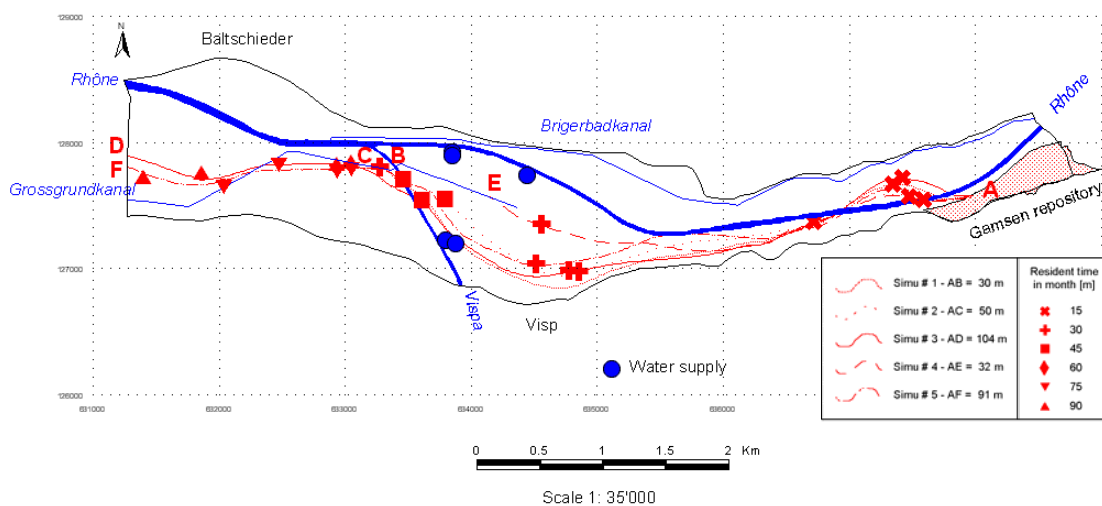


Figure 7 : Visualization of 5 tracer pathlines issuing from a single point source (A). Travel distances at 15-monthes intervals are also indicated along each pathline, using a distinct symbol for each pathline. The 5 pathlines correspond to 5 groundwater flow patterns calculated with the 5 conditional replicates of log-transmissivity.

Fig. 7 synthetizes the influence of the spatial variability of the transmissivity on the groundwater flows systems. It shows five tracer pathlines issuing from a single point source (A). Points B, C, D, E and F represent discharge zones. Travel distances at 15-monthes intervals are also indicated along each pathline, using a distinct symbol

for each pathline. The five pathlines correspond to five groundwater flow patterns calculated with the five conditional replicates of log-transmissivity.

Trajectory dispersal is apparent from the data. The distance traveled by a pollutant particle over 30 months varies between 3150 m and 4800 m over five different but equally plausible scenarios (conditional simulations). The uncertainty is about 42% relative to the average travel distance, or 55% relative to the smallest travel distance mentioned above. This result is important for groundwater catchment protection (see Fig. 7, location of water supply).

## 4. CONCLUSIONS

As main result of this study, we show that the uncertainty of the results in terms of pollutant migration can be relatively important and that the probabilistic approach is a good means to estimate this uncertainty. Our immediate purpose in this preliminary study was not to conduct a complete probabilistic analysis of the possible trajectories, but only to assess roughly the importance of uncertainties in predictions of pollutant migration, given the available data. Conversely, these uncertainties measure, in a sense, the information content of our dataset in terms of pollutant transport. With this in mind, we constructed and analyzed only five simulations – rather than the hundreds or thousands that would be required for a full Monte-Carlo analysis of the pollution migration problem. In spite of this limitation, our study clearly shows what type of results can be obtained with the probabilistic approach. For instance, it was found that the distance traveled by a pollutant particle during 30 months varies between 3150 m and 4800 m over the five different (but equally plausible) conditional simulations. The

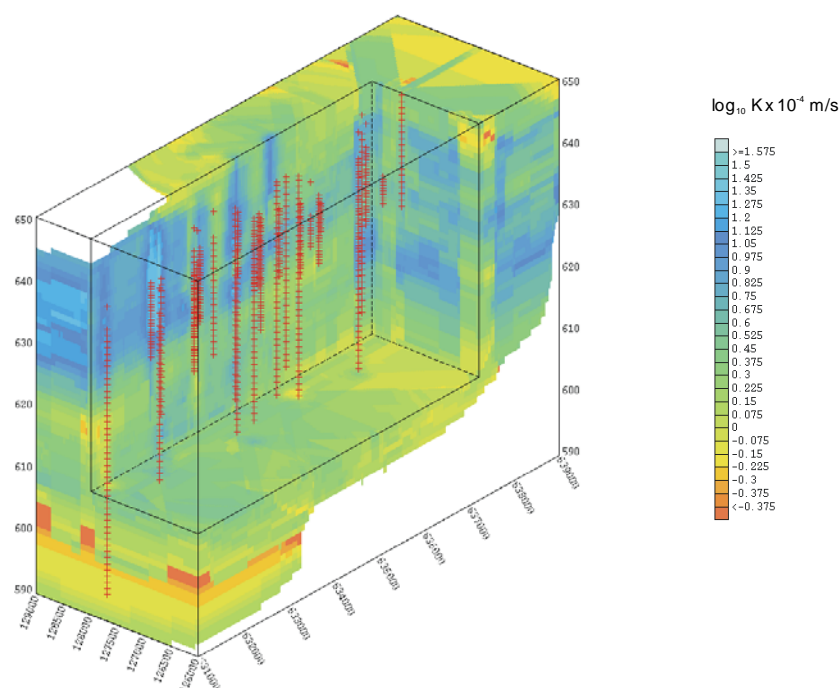


Figure 8 : 3-D color display of estimated log-permeability distribution obtained from flowmeter measurements within the Visp area, Valais, Switzerland (Rhône valley). The color shading indicates values of  $\log_{10}K \times 10^{-4}$  m/s estimated by standard kriging with an omnidirectional variogram (*Isatis 3*). The (x, y, z) estimation grid is 25m x 25m x 1m. The crosses indicate the (x, y, z) positions of the 791 values of flowmeter measurements.

uncertainty amongst the five different transport scenarios is therefore about 42% relative to the average travel distance, or 55% relative to the smallest travel distance. It should be emphasized that the probabilistic approach is particularly relevant in the case at hand, as it answers the new swiss requirements of water catchment protection (see introduction). Our conclusion is that an extensive analysis of uncertainty and risk is feasible in this probabilistic framework, and that such an analysis should accompany any serious study on pollution migration and remediation. Another important point is that our probabilistic approach is geostatistically-based, that is, it uses spatial statistics. It is therefore well adapted to the formulation of optimal estimation (kriging) and uncertainty analysis of multidimensional, spatially distributed groundwater pollution problems.

## 5. FUTURE WORK

The methods mentioned above can be extended to conduct a joint estimation of hydraulic heads  $H$  and aquifer transmissivities  $T$  by exploiting the spatial cross-correlation between  $T$  and  $H$  (co-kriging). This technique should further improve the estimation of  $T$  via  $(T, H)$  correlations, since  $H$  data (piezometers) are more easily acquired than transmissivity or permeability data (well tests, borehole flowmeter tests, etc). However, the co-kriging technique can be implemented only if one knows "in advance" the  $(T, H)$  cross-correlation function between  $T$ . Several authors propose geostatistical co-kriging approaches based on stochastic models of the  $(T, H)$  spatial correlation structure, on more or less physical grounds [Mizell 1980; Dagan 1985; Gelhar 1993; Dong 1990; Roth 1997]. In some of these works, the groundwater flow is used to obtain the  $(T, H)$  correlation structure. The resulting co-kriging estimation scheme is then equivalent to solving an inverse groundwater flow problem (with probabilistic regularization). In future, we intend to treat the pollution problem in 3-D (by combination of 2D and 3D permeability data measured on different scales; taking

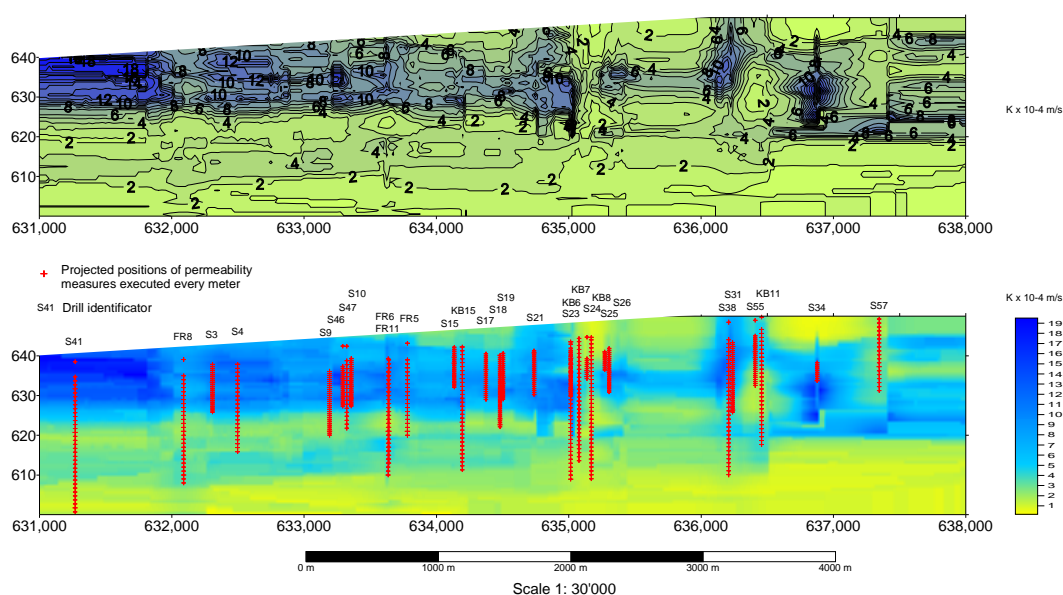


Figure 9 : Visualization of a 2-D vertical cross-section of permeability  $K(x, z)$ , extracted and transformed from the kriged 3D log-permeability field  $K(x, y, z)$ . The top view shows isovalue contours of  $K \times 10^{-4}$  m/s, while the bottom view displays a color-coded map of the same. This cross-sectional permeability map is to be compared with the lithologic profile of figure 1.

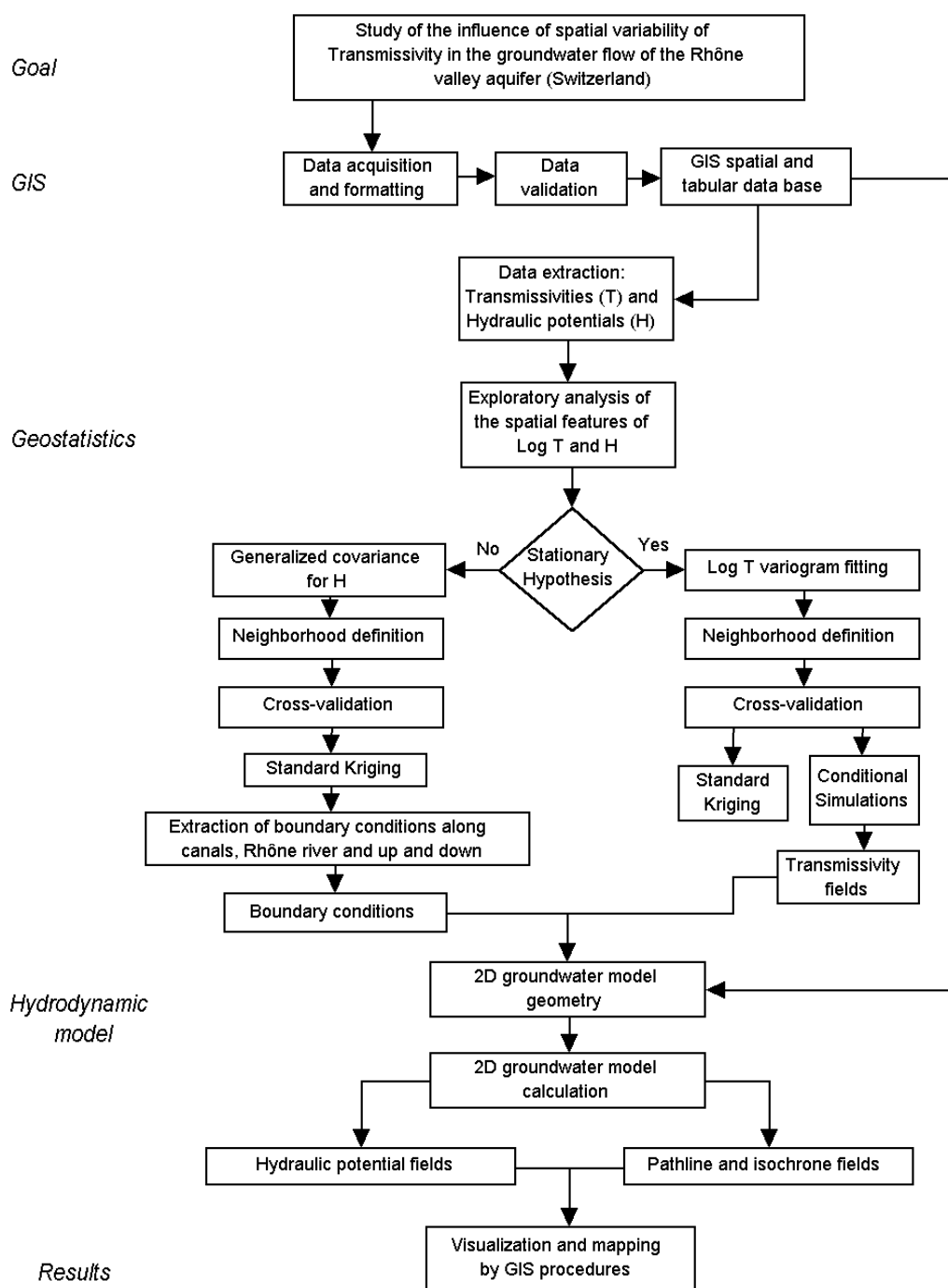
into account K-H correlation) by generating 3D geostatistical simulations of the permeability field  $K(x,y,z)$  based on 791 values obtained by flowmeter measurements at every meter depth increment ( $z_i$ ) in 30 different drillings ( $x_i,y_i$ ). Figure 8 shows a 3D block diagram representing the log-permeability ( $\log_{10}K$ ) distribution estimated by standard kriging. Figure 9 shows a cross-section of the kriged permeabilities extracted from the 3D block diagram of Fig. 8. This permeability cross-section (Fig. 9) can be used as a hydro-lithologic model, to be substituted to the classical lithologic model shown earlier in Fig.1.

**Acknowledgments :** This study was funded by the Swiss National Foundation for Scientific Research (research project N° 21-39357.93 and 20-47064.96)

## 6. REFERENCES

- Ababou R., Amvrossios C., Bagtzoglou E., Wood F., 1994. *On the Condition Number of Covariance Matrices in Kriging Estimation and Simulation of Random Fields*. Mathematical Geology, Vol. 26, p. 99-133.
- Bouzelboudjen M., Király L., 1989. *Modélisation tridimensionnelle de la nappe phréatique de la plaine du Rhône à Viège*. Troisièmes Journées Valaisannes des Sciences Naturelles, Suisse, avril 1989. Bulletin Murithienne 107, p. 69-74.
- Chauvet P., 1992. *Traitement des données à support spatial : la géostatistique et ses usages*. Centre de Géostatistique, Ecole des mines de Paris, Fontainebleau, France, 43 p.
- Chilès J.P. & Delfiner P., 1999. *Geostatistics : modelling spatial uncertainty*. Wiley Series in Probability and Mathematical Statistics, 695 p.
- Cressie N., 1993. *Statistics for spatial data*, Wiley, New York.
- Dagan G., 1985. *Stochastic modeling of groundwater flow by unconditional and conditional probabilities, the inverse problem*. Water Resour. Res., 21 (1), p. 65-72.
- Delhomme, J.P, 1979. *Spatial Variability and Uncertainty in Grounwater Flow Parameters : A geostatistical Approach*. Water Resources Research 15 (2), p. 269-280.
- Diersch H.-J. G. & al., 1999. *Interactive, graphics-based finite-element simulation system Feflow for modeling groundwater flow, contaminant mass and heat transport processes*. User's manual version 4.8, WASY Institute for water resources planning and system research Ltd Berlin.
- Dong A., 1990. *Estimation géostatistique des phénomènes régis par des équations aux dérivées partielles*. Thèse de Docteur en Géostatistique, Ecole des Mines de Paris, Fontainebleau, 262 p.
- Gelhar L.W., 1993. *Stochastic subsurface hydrology*. Prentice Hall, Englewood Cliffs NJ.
- Geostatistics, 1998. Isatis 3, The Geostatistical key. User's Guide, Avon, France.

- Jaquet O., Ornstein P., Rey M., Rouiller J.-D., Bouzelboudjen M., 2000. *Optimisation géostatistique de réseaux de mesures piézométriques : le cas de la nappe alluviale dans la vallée alpine du Rhône, Suisse*. Bull. d'Hydrogéol. de Neuchâtel No 18 : p. 77-98, Editions Peter Lang, Berne.
- Kimmeier F., Bouzelboudjen M., Perrochet P., 2000. *Simulations numériques 2-D et 3-D des écoulements souterrains saturés et non saturés en nappe libre pour les états permanent et transitoire dans la région de Baltschieder-Gamsen*. Centre d'hydrogéologie, Université de Neuchâtel, 26 p., 37 fig., 8 tab., rapport inédit.
- Kitanidis P.-K., 1997. *Introduction To Geostatistics. Applications in Hydrogeology*. Cambridge University Press, 249 p.
- Matheron G., 1970. *La théorie des variables régionalisées et ses applications*. Centre de Géostatistique, Ecole des Mines de Paris, Fascicule 5, 211 p.
- Mizell S.A., 1980. *Stochastic flow analysis of spatial variability in two-dimensional groundwater flow with implications for observation-well-network design*. PhD, New Mexico Institute of Mining and Technology, Socorro, New Mexico.
- Ribeiro L.T., Muge F.H., 1989. *A Geostatistical Approach to the Modelling of a Piezometric Field*. M. Armstrong (ed.), Geostatistics, Vol. 2, p. 651-660. Kluwer Academic Publisher.
- Rossier, Y., 1990. *Simulation de la pollution de la nappe du Rhône en amont de Viège (Vs) : problèmes et résultats*. Bull. d'Hydrogéol. N° 9, p. 13-8. , Editions Peter Lang, Berne.
- Roth C., de Fouquet C., Chilès J.-P., Matheron G., 1997. *Geostatistics applied to hydrogeology's inverse problem : taking boundary conditions into account*. In E.Y. Baafi et N.A. Schofield, Geostatistics Wollongong '96, Kluwer Academic Publishers, Dordrecht, vol. 2, p. 1085-1097.
- Rouhani S., Geogakakos A.P., Kitanidis P.K., Loaiciga H.A, Olea R.A, Yates S.R., 1990. *Geostatistics in geohydrology : Part I*. Basic concepts, ASCE J. of Hydraulic Engineering, 116 (5), p. 612-632.
- Rouhani S., Geogakakos A.P., Kitanidis P.K., Loaiciga H.A, Olea R.A, Yates S.R., 1990. *Geostatistics in geohydrology : Part II*. Applications, ASCE J. of Hydraulic Engineering, 116 (5), p. 633-658.
- Schafmeister M.-TH, Pekdeger A., 1992. *Spatial structure of hydraulic conductivity in various porous media - problems and experiences*. Soares Amilcar (eds.), Geostatistics Troia'92. Vol. 2, p. 734-744.
- Tompson, A.F.B., Ababou R., and Gelhar L. W., 1989. *Implementation of the three-dimensional turning bands random field generator*, Water Resources Res., 25 (10), p. 227-243.
- Vassolo S., Kinzelbach W., Schäfer W., 1998. *Determination of a well head protection zone by stochastic inverse modelling*. J. Hydrology Vol. 206, p. 268-280.
- Corresponding author** : Francesco Kimmeier, Institut de Géologie, Centre d'Hydrogéologie, Université de Neuchâtel, 11 rue Emile-Argand, 2007 Neuchâtel.  
Tél : +4132/718.26.30 - Fax : +4132/718.26.03  
E-mail : francesco.kimmeier@unine.ch



Annex 1 : Flow chart of the study